NASA/TM—2001-210562

Gust Response Analysis of a Turbine Cascade

R.S.R. Gorla
Cleveland State University, Cleveland, Ohio

T.S.R. Reddy
The University of Toledo, Toledo, Ohio

D.R. Reddy and A.P. Kurkov
Glenn Research Center, Cleveland, Ohio

Prepared for the
46th International Gas Turbine and Aeroengine Technical Congress,
Exposition, and Users Symposium
sponsored by the American Society of Mechanical Engineers
New Orleans, Louisiana, June 4–6, 2001

National Aeronautics and
Space Administration

Glenn Research Center

January 2001

Acknowledgments

One of the authors (RSRG) is grateful to Dr. Shantaram S. Pai, Mr. Jeff Rusick, and Mr. Oral Mehmed of NASA Glenn Research Center for their interest and financial support.

Available from

NASA Center for Aerospace Information
7121 Standard Drive
Hanover, MD 21076
Price Code: A03

National Technical Information Service
5285 Port Royal Road
Springfield, VA 22100
Price Code: A03

Available electronically at http://gltrs.grc.nasa.gov/GLTRS

GUST RESPONSE ANALYSIS OF A TURBINE CASCADE

R.S.R. Gorla
Department of Mechanical Engineering
Cleveland State University
Cleveland, Ohio 44115

T.S.R. Reddy
Department of Mechanical Engineering
The University of Toledo
Toledo, Ohio 43606

D.R. Reddy and A.P. Kurkov
National Aeronautics and Space Administration
Glenn Research Center
Cleveland, Ohio 44135

SUMMARY

A study was made of the gust response of an annular turbine cascade using a two-dimensional Navier Stokes code. The time-marching CFD code, NPARC, was used to calculate the unsteady forces due to the fluid flow. The computational results were compared with a previously published experimental data for the annular cascade reported in the literature. Reduced frequency, Mach number and angle of incidence were varied independently and the gust velocity was sinusoidal. For the high inlet velocity case, the cascade was nearly choked.

NOMENCLATURE

A,B	amplitudes
C_h	blade chord length
M	Mach number
N	number of cylinders
p	static pressure
S	blade spacing
T	temperature
U_1	axial inlet velocity
t	time
u,v	axial and tangential velocity components
x,y	axial and tangential coordinate directions

Greek Symbols:

α	phase angle
β	incidence
ϕ	flow coefficient
ρ	density
σ	solidity (C_h/S)
ω_h	angular velocity

Subscripts:

1	inlet conditions
2	conditions downstream of rotor

w rotor conditions
r radial conditions
h blade properties

INTRODUCTION

Periodic wake-passing from upstream blade rows in the gas turbine flow field strongly influences the unsteady forces on the surfaces of the downstream blades. Manwaring and Wisler (1993) conducted a series of experiments involving a gust inlet velocity in a large speed compressor and turbine rig and provided aerodynamic forced response measurements on downstream stators. Kurkov and Lucci (1997) provided experimental data on a gust response of an annular turbine cascade in a transonic flow regime. They varied the reduced frequency, Mach number and incidence angle independently. The mean flow was documented by measuring blade surface pressures and cascade exit flow.

The unsteady aerodynamics generated by a strong blade row coupling and the interactions due to the highly unsteady flow induce vibrations, which can lead to high cycle fatigue. In order to predict blade life or design blades for longer high cycle fatigue life, accurate predictions of the multiblade row unsteady aerodynamics are crucial. Turbomachinery aeroelastic analyses have been carried out at NASA Glenn Research Center for the past decade. Kielb and Chiang (1992) reviewed research related to the forced response analyses of turbomachinery. Hall and Verdon (1990) provided an analysis for gust response for cascades. Giles (1988) computed the interaction of an unsteady wake with a rotor. Reddy and Srivastava (1994) presented an analysis of a rotor-stator stage interaction by solving Euler equations. Reddy and Srivastava (1996) extended their previous work to include the effects of incoming gust. Barter et al. (2000) studied the interaction effects in a transonic turbine stage by means of a three-dimensional, viscous, time-accurate computational code. Their results showed that interaction effects must be taken into account in order to accurately predict the unsteady loading on the upstream blade row. Haldeman et al. (2000) reported a combined experimental and computational effort quantifying unsteady airfoil interactions.

The present work was undertaken in order to study the fluid/structure interaction for the turbomachinery blade configuration using the state of the art CFD techniques. The time-marching CFD code, NPARC was used to calculate the unsteady forces due to the fluid flow. The computational results are compared with the experimental data of Kurkov and Lucci (1997).

GOVERNING EQUATIONS

The differential equations used are the Reynolds mass-averaged Navier-Stokes equations inside a rotating blade passage and may be written as:

$$\rho_{,t} + (\rho U_i)_{,i} = 0$$

$$(\rho U_i)_{,t} + (\rho U_i U_j)_{,j} + 2\rho\varepsilon_{ijk}\Omega_j U_k = -p_{,i} + \left[\mu\left(U_{i,j} + U_{j,i} - \frac{2}{3}U_{k,k}\delta_{ij}\right) - \rho\overline{u_i u_j}\right]_{,j} + F_i$$

$$(\rho e - p)_{,t} + (\rho U_i e)_{,j} = \left[\left(\frac{\mu}{\mathrm{Pr}}\right)_{eff} T_{,j}\right]_{,j} - (pU_j)_{,j} + U_i F_i + \left[U_i\mu\left(U_{i,j} + U_{j,i} - \frac{2}{3}U_{k,k}\delta_{ij}\right)\right]_{,j}$$

$$p = \rho RT$$

where U_i = mean velocity, u_i = fluctuating velocity, e = total energy, Ω_i = angular velocity. For stationary blades, we set $\Omega_i = 0$. It is well known that neither the conventional mixing length type turbulence model nor any standard two-equation type turbulence model describes turbulence stresses properly in the region behind a shock wave or in the separated flow regions. Several recent studies have shown that significant improvement can be achieved when the standard two-equation model is modified to include the low Reynolds number effects. The following are the transport equations for the turbulent shear stress:

$$(\rho k)_{,t} + (\rho U_j k)_{,j} = \left(\frac{\mu_{eff}}{\sigma_k} k_{,j}\right)_{,j} + \rho\left[\overline{u_i u_j}\right] U_{ji} - \rho\varepsilon - \frac{2\mu k}{l^2}$$

$$(\rho\varepsilon)_{,t} + (\rho U_i \varepsilon)_{,j} = \left(\frac{\mu_{eff}}{\sigma_\varepsilon} \varepsilon_{,j}\right)_{,j} + C_1 \frac{\rho\varepsilon}{k}\left[\overline{u_i u_j} U_{j,i}\right] - \frac{\rho\varepsilon}{k}\left(C_2 f\varepsilon + \frac{2\nu k \exp(-C_4 u^* l / \nu)}{l^2}\right)$$

Standard expressions were used for μ_{eff}, f and C's. These details are omitted in order to conserve space. The mean flow and turbulence equations were integrated in time using a fully coupled approximately factored implicit backward Euler method.

CODE DESCRIPTION

Two-dimensional time-marching flow simulations were performed with NPARC version 3.1 code. NPARC solves the Euler or Navier-Stokes equations in conservation law form on a multi block body fitted grid system. The fluid is assumed to be ideal and Newtonian and the Fourier heat conduction law is assumed for heat transfer. The flow can be assumed to be laminar, turbulent or inviscid. A variety of turbulence models, including the k-ε model can be selected. The flow simulations were performed in two steps. First, a converged steady state flow solution was achieved. In the second step, a convective gust perturbation of known strength was introduced at the upstream boundary and allowed to propagate down the cascade. The steady state simulation to initialize the flow field was done with the approximate factorization algorithm (ISOLVE = 1) using local time stepping (IVARDT = 2) with DTCAP = 1. Typically, about 2500 time steps were required to reduce the L_2 norm to about 10^{-7}. For the time accurate computations, a five step Jameson algorithm second order accurate in time was selected (ISOLVE = 5). The time step throughout the grid block was set to a constant equal to the CFL limit specified by DTCAP (IVARDT = 4 and DTCAP = 0.3) at the location of maximum change in the flow variables.

GRID GEOMETRY DESCRIPTION AND BOUNDARY CONDITIONS

Figure 1 shows a single grid block used for computations. The airfoil upper and lower surfaces are located along lines BC and FG, respectively where solid wall boundary conditions are prescribed. Lines AE and DH represent inflow and outflow boundaries, respectively. The flow incidence angle is specified and the backpressure is adjusted until the average Mach number along the inflow boundary AE matches a specified value. Periodicity is imposed between lines AB and EF and lines CD and GH.

Computational grids were generated using the GRIDGEN2D grid generation program. A uniform grid spacing was used in each coordinate direction. A grid refinement study was completed to ensure that the computed results were independent of the grid density. A grid of 41×118 was selected for the cascade simulation. There were 60 points on the airfoils, 29 points between the inlet and leading edge and the rest between the trailing edge and exit plane.

For treating the velocity perturbations, namely, the gust for the present problem, the wake profile was fitted to experimental velocity profile at the inlet in the following form:

$$\frac{u}{U_1} = \left\{1 + \mathrm{ASin}\left[N_w\left(\frac{y}{R} + \omega t\right) + \alpha_1\right]\right\}$$

$$\frac{v}{U_1} = \left\{1 + \mathrm{BSin}\left[N_w\left(\frac{y}{R} + \omega t\right) + \alpha_2\right]\right\}$$

In the above equations, A and B are the amplitudes; U_1 the axial inlet velocity and α_1 and α_2 the phase angles.

DESCRIPTION OF THE EXPERIMENTAL SETUP

The air entered the bellmouth and passed through the annulus to the rotor consisting of radial pins, either 0.317 or 0.476 cm (1/8 or 3/16 in.) in diameter. The wakes from the pins were convected by the main flow into a turbine cascade. The rotor pins and the turbine cascade are shown in figure 2. The rotor induced a swirl of 3 to 5° into the mean flow. The cascade turning angle was 61°, the blade chord angle relative to the axial direction was 38° and the distance between the rotor and the cascade leading edge was 3.9 axial chords. The chord length was 4.75 cm and annulus outside and inside diameters were 40.64 and 27.13 cm, respectively. The cascade consisted of 23 blades that extended in the radial direction spanning the annulus. The power was delivered to the rotor through a long shaft that extended vertically through the inner pipe of the annulus. The shaft exits the outer pipe at the 90°-bend close to the floor level and is terminated by a belt-driven pulley, which transmits the power from the electric motor.

The number of pins on the rotor was varied among 24, 12 and 6. The pin diameter for the 24-pin configuration was 0.317 cm and for 12 and 6-pin configurations, it was 0.476 cm. The pin diameter was increased for the last two configurations in order to reduce the number of harmonics in the wake. The reduced frequency $\omega = \frac{N_w \omega_r c_h}{U_1} = 0.375 \frac{N_w}{\phi}$ was varied by changing the number of pins on the rotor, N_w. Here, ω_r is the shaft angular velocity, c_h the blade chord, U_1 the axial inlet velocity and ϕ the flow coefficient. Subscript 1 denotes the station downstream of the bellmouth and upstream of the rotor. The reduced frequency values were 10, 5 and 2.5 for the available values of N_w. The inlet Mach number was either 0.2 or 0.27. At the higher inlet Mach number the flow in the blade passage throat was near choking at the midspan radius. The flow coefficient was kept constant at 0.9 and the shaft speeds for the two Mach numbers were 4290 and 5790 rpm. The Reynolds numbers corresponding to low and high inlet velocities were 2.7×10^5 and 3.6×10^5, respectively based on the blade chord. Positive and negative values of incidence correspond to two directions of rotation.

The inlet condition was defined by the barometric pressure, inlet temperature at the bellmouth inlet and several static pressure measurements on the inside and outside wall of the annulus downstream of the bellmouth. The cascade exit flow was surveyed at the blade midspan radius over a circumference in excess of one blade pitch with a five-hole probe. This station was one axial chord length downstream of the cascade trailing edge. The locations of the steady state and dynamic ports on the instrumented blades are shown in figure 3. Kurkov and Lucci (1997) have documented in more detail the measurements taken.

RESULTS AND DISCUSSION

Figure 4 displays the steady state results for the pressure coefficient distribution for inlet Mach number $M_1 = 0.2$ and inlet angle of attack of 4.59°. Figure 5 shows the steady state results for the pressure coefficient distribution for inlet Mach number $M_1 = 0.27$ and inlet angle of attack of 5.17°. The computed results agree with the experimental data quite well in both cases. The spikes in the pressure coefficient distribution in the vicinity of the trailing edge may be due to the definition of the airfoil surface coordinates in generating the grid.

Figures 6 to 9 show results for the distribution of the amplitude of the unsteady pressure coefficient (percentage of the inlet dynamic head) for inlet Mach number $M_1 = 0.2$ and reduced frequency of 10 based on chord length. Figures 10 to 13 show results for the distribution of the amplitude of the unsteady pressure coefficient for inlet Mach number $M_1 = 0.27$ at the same reduced frequency. The computed results agree with the experimental results within 20 percent error over most of the blade length, both on the suction and the pressure surfaces. However, in the vicinity of the leading edge of the blade, the discrepancy seems to be higher.

Figures 14 to 17 show results for the distribution of the phase angle for inlet Mach number $M_1 = 0.2$ and reduced frequency of 10. Figures 18 to 21 show the same results for inlet Mach number $M_1 = 0.27$. The quantitative agreement between the computed and measured values of the phase angle is poor although qualitatively they are showing similar trends.

CONCLUDING REMARKS

In this paper, we have considered an annular cascade configuration subjected to unsteady gust inflow conditions. The gust response calculation has been implemented into the time marching CFD code, NPARC. The computed steady state results for the pressure distribution demonstrated good agreement with experimental data. The computed results for the amplitudes of the unsteady pressure over the blade surfaces agreed with experimental data within 20 percent error margin, except in the vicinity of leading edge. There exists considerable quantitative discrepancy between the computed and experiments results for phase angle, although the trends are similar.

REFERENCES

Barter, J.W., Vitt, P.H. and Chen, J.P., 2000: "Interaction Effects in a Transonic Turbine Stage," 2000–GT–0376, ASME Turbo Expo, Munich, Germany.

Giles, M.B., 1988: "Calculation of Unsteady Wake/Rotor Interactions," Journal of Propulsion and Power, Vol. 4, pp. 356–362.

Hall, K.C. and Verdon, J.M., 1990: "Gust Response Analysis for Cascades Operating in Nonuniform Mean Flows," Unsteady Aerodynamic Phenomena in Turbomachines, AGARD-CP–468, Paper No. 10.

Haldeman, C.W., Dunn, M.G., Abhari, R.S., Johnson, P.D. and Montesdeoca, X.A., 2000: "Experimental and Computational Investigation of the Time-Averaged and Time-Resolved Pressure Loading on a Vaneless Counter-rotating Turbine," 2000–GT–0445, ASME Turbo Expo, Munich, Germany.

Kielb, R.E. and Chiang, H.D., 1992: "Recent Advances in Turbomachinery Forced Response Analyses," AIAA 92–0012, 30th Aerospace Sciences Meeting & Exhibit, Reno, NV.

Kurkov, A.P. and Lucci, B.L., 1997: "Measurement of Gust Response on a Turbine Cascade," ASME Journal of Turbomachinery, Vol. 119, pp. 238–246.

Manwaring, S.R. and Wisler, D.C., 1993: "Unsteady Aerodynamics and Gust Response in Compressors and Turbines," ASME Journal of Turbomachinery, Vol. 115, pp. 724–740.

Reddy, T.S.R. and Srivastava, R., 1994: "Analysis of a Rotor-Stator Stage Using a Two Dimensional Euler Aeroelatic Solver," AIAA–94–1638, 35th Structures, Structural Dynamics and Materials Conference, Hilton Head, S.C.

Reddy, T.S.R. and Srivastava, R., 1996: "Gust and Structural Response Analysis of a 2D Cascade Using an Euler Aeroelatic Solver," AIAA–96–1492, 37th Structures, Structural Dynamics and Materials Conference, Salt Lake City, UT.

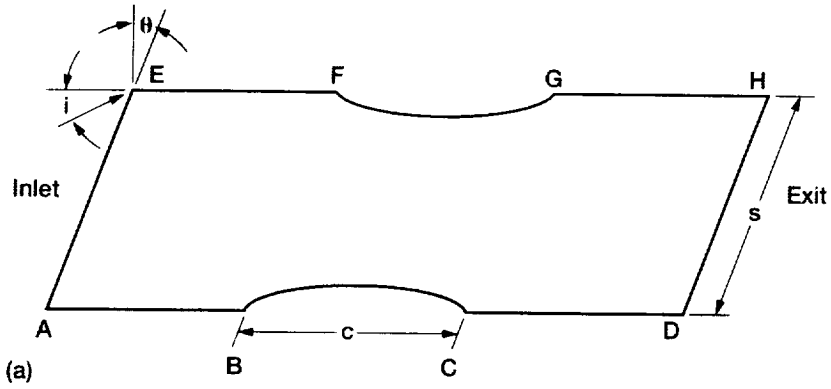

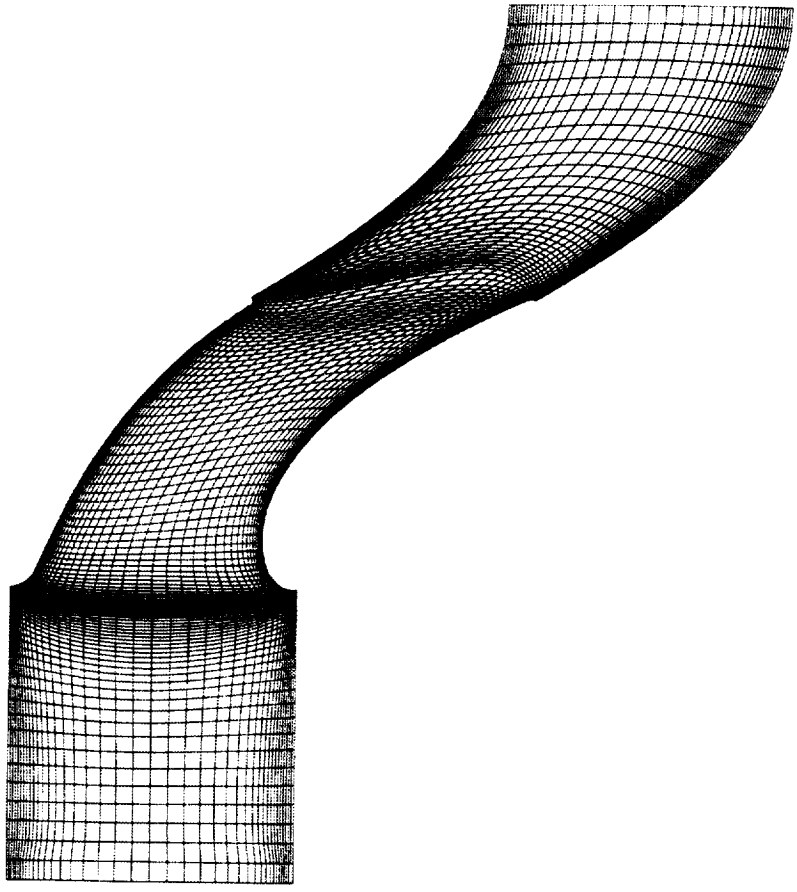

Figure 1.—(a) Cascade geometry for a single blade passage. (b) Grid.

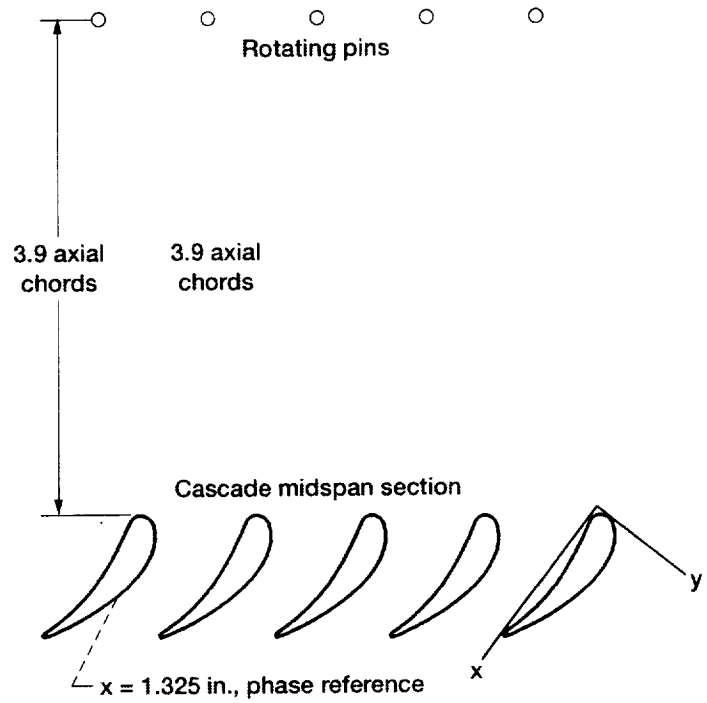

Figure 2.—Experimental setup.

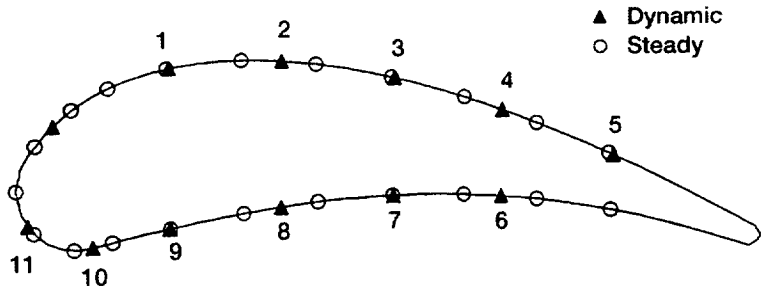

Figure 3.—Instrumentation ports.

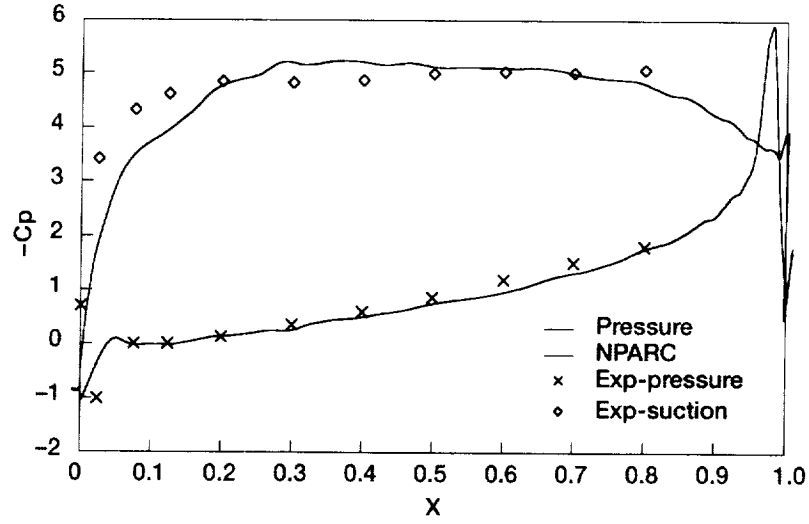

Figure 4.—Steady state pressure prediction (M_1 = 0.2, i = 4.59°).

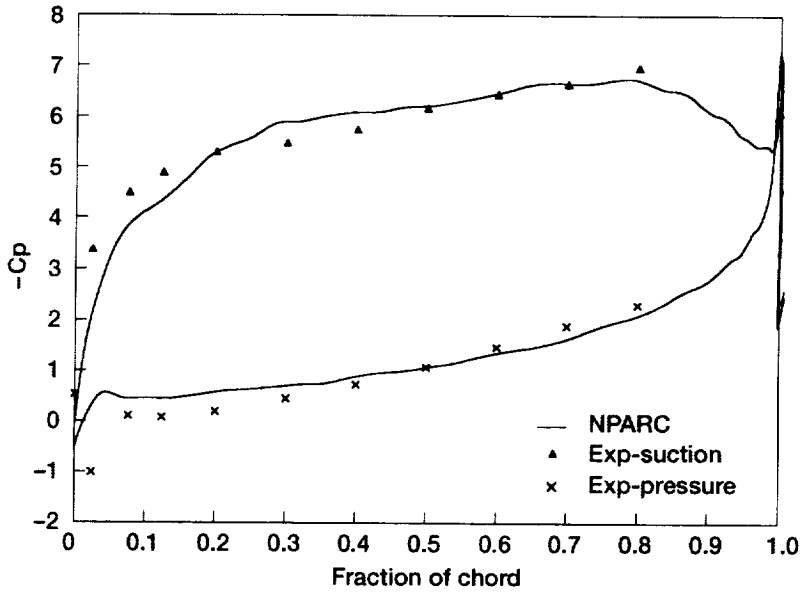

Figure 5.—Steady state pressure prediction (M_1 = 0.27, i = 5.17°).

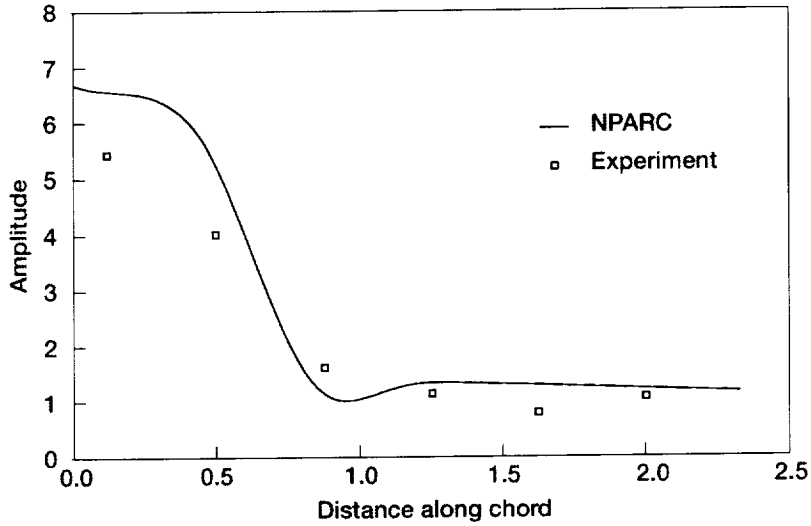

Figure 6.—Amplitude of the unsteady pressure coefficient distribution on suction surface (M_1 = 0.2, i = 3.24°).

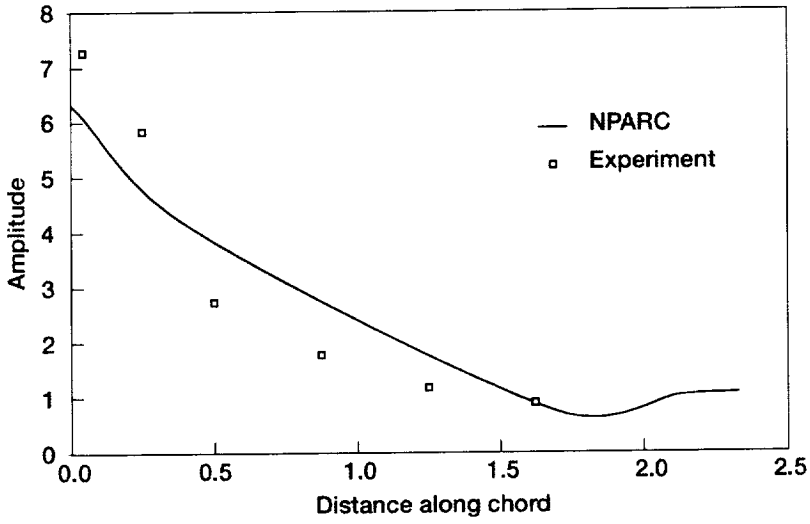

Figure 7.—Amplitude of the unsteady pressure coefficient distribution on pressure surface (M_1 = 0.2, i = 3.24°).

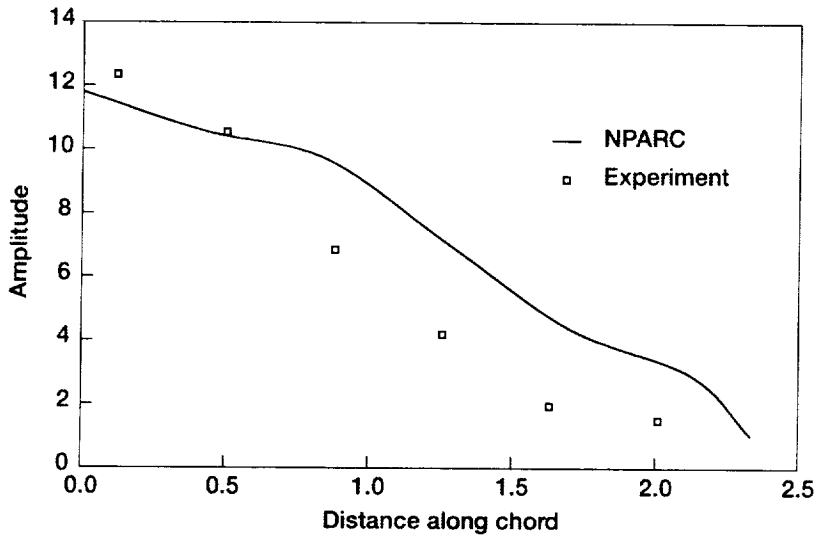

Figure 8.—Amplitude of the unsteady pressure coefficient distribution on suction surface (M_1 = 0.2, i = 3.24°).

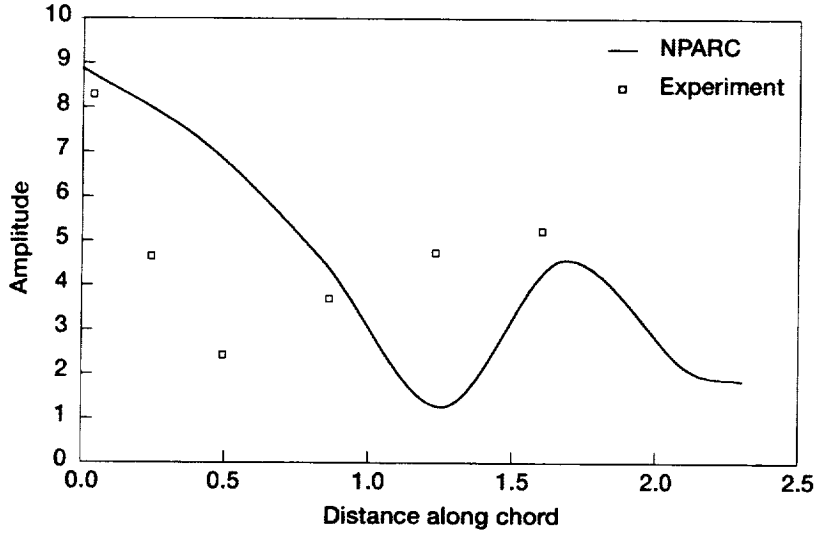

Figure 9.—Amplitude of the unsteady pressure coefficient distribution on pressure surface (M_1 = 0.2, i = 3.24°).

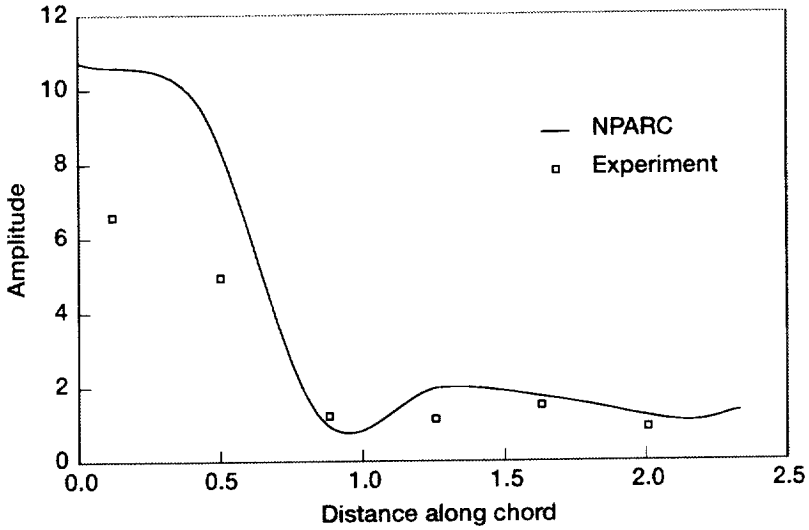

Figure 10.—Amplitude of the unsteady pressure coefficient distribution on suction surface (M_1 = 0.27, i = 2.98°).

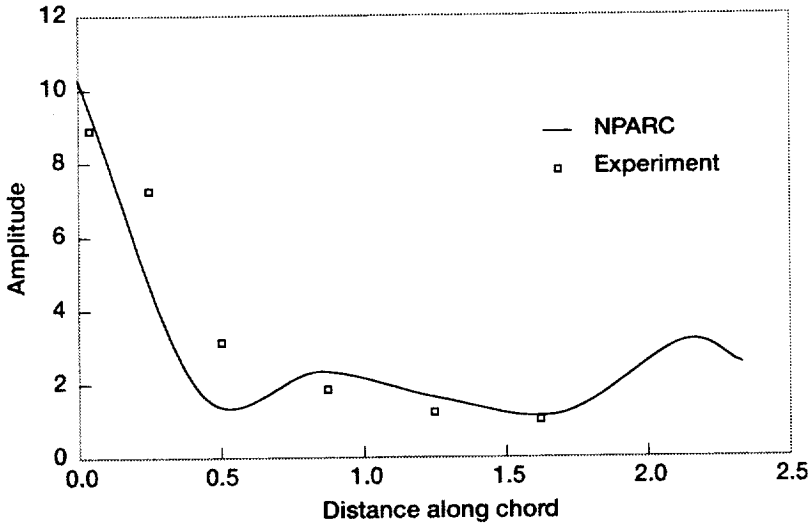

Figure 11.—Amplitude of the unsteady pressure coefficient distribution on pressure surface (M_1 = 0.27, i = 2.98°).

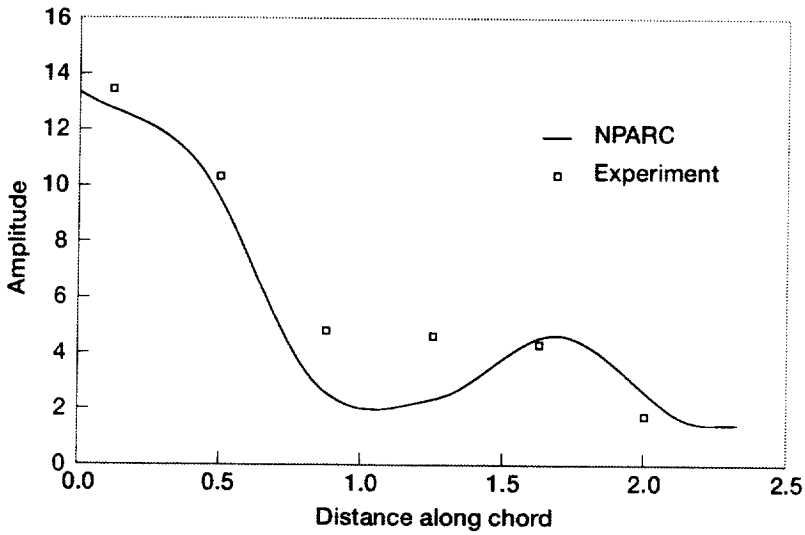

Figure 12.—Amplitude of the unsteady pressure coefficient distribution on suction surface (M_1 = 0.27, i = 2.98°).

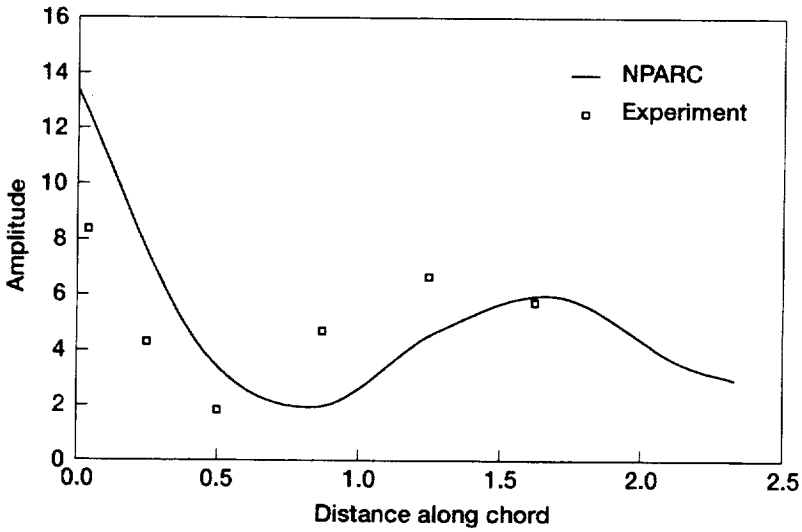

Figure 13.—Amplitude of the unsteady pressure coefficient distribution on pressure surface (M_1 = 0.27, i = 2.98°).

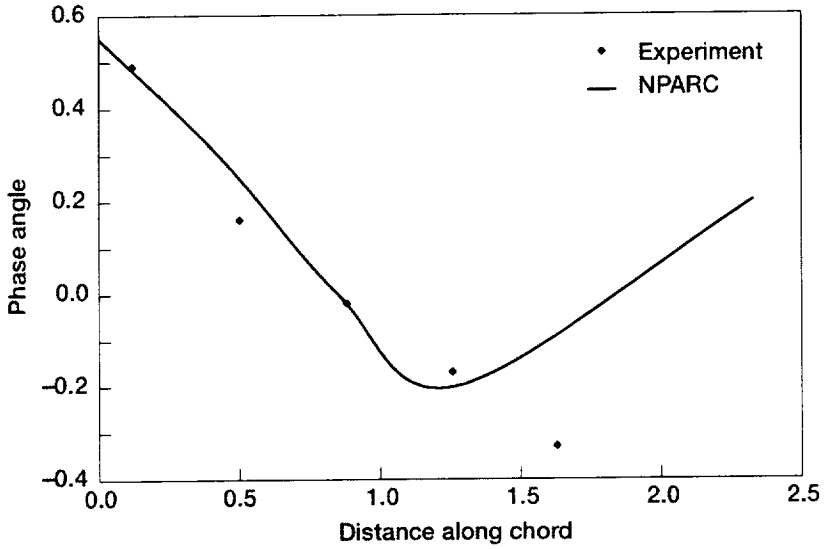

Figure 14.—Phase angle distribution on suction surface (M_1 = 0.2, i = 3.24°).

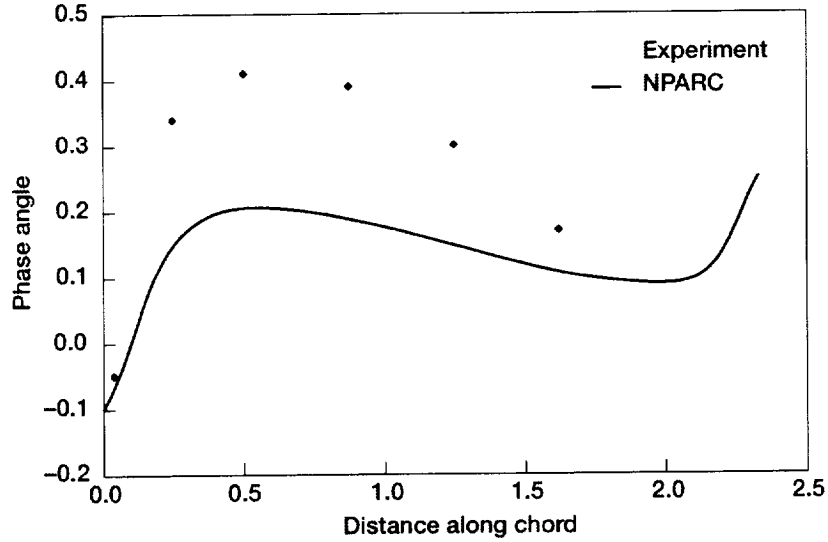

Figure 15.—Phase angle distribution on pressure surface (M_1 = 0.2, i = 3.24°).

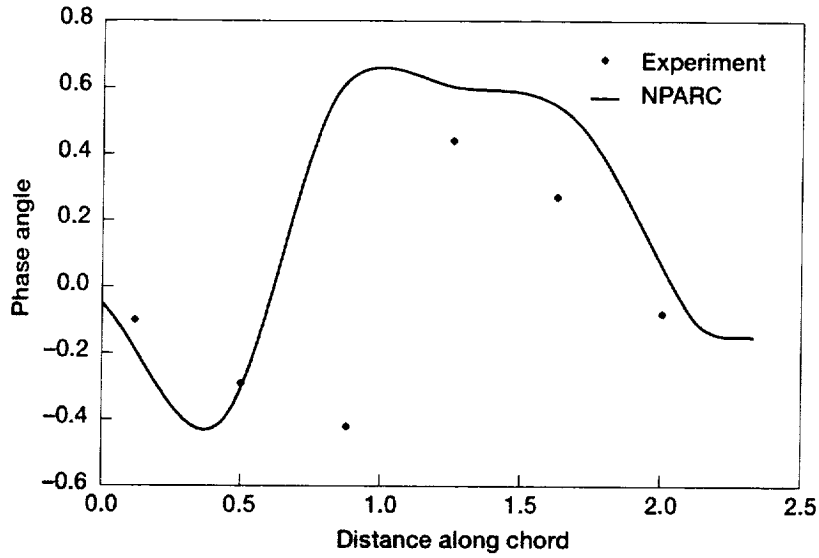

Figure 16.—Phase angle distribution on suction surface (M_1 = 0.2, i = 3.24°).

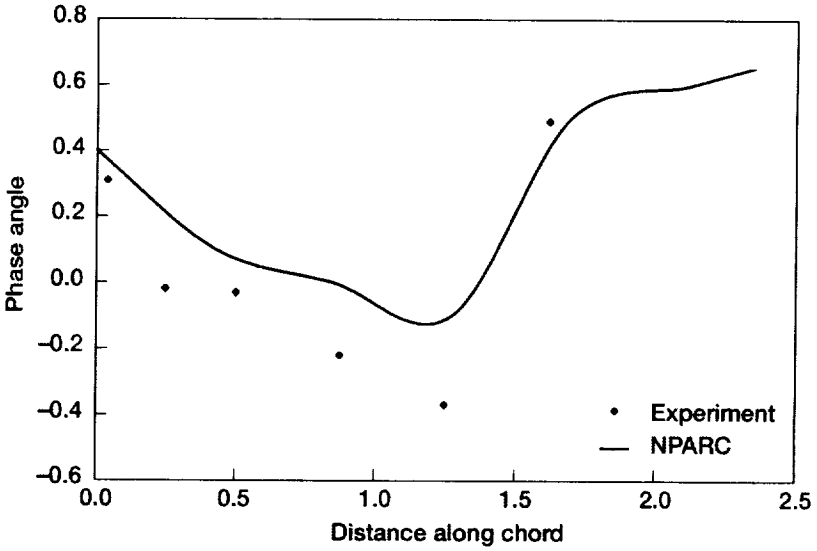

Figure 17.—Phase angle distribution on pressure surface (M_1 = 0.2, i = 3.24°).

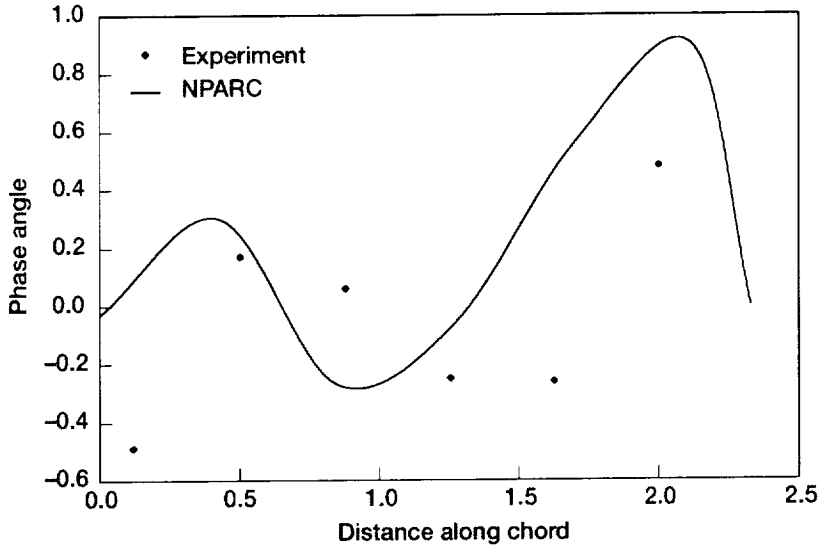

Figure 18.—Phase angle distribution on suction surface (M_1 = 0.27, i = 2.98°).

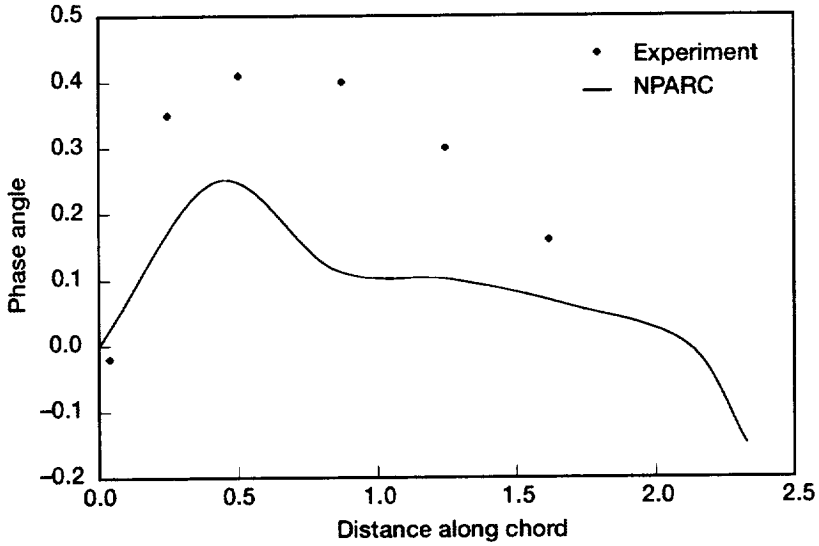

Figure 19.—Phase angle distribution on pressure surface (M_1 = 0.27, i = 2.98°).

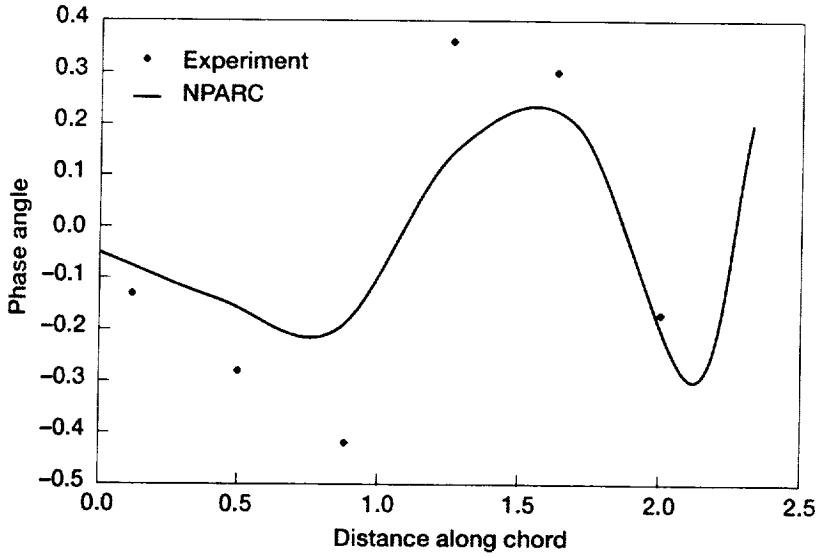

Figure 20.—Phase angle distribution on suction surface (M_1 = 0.27, i = 2.98°).

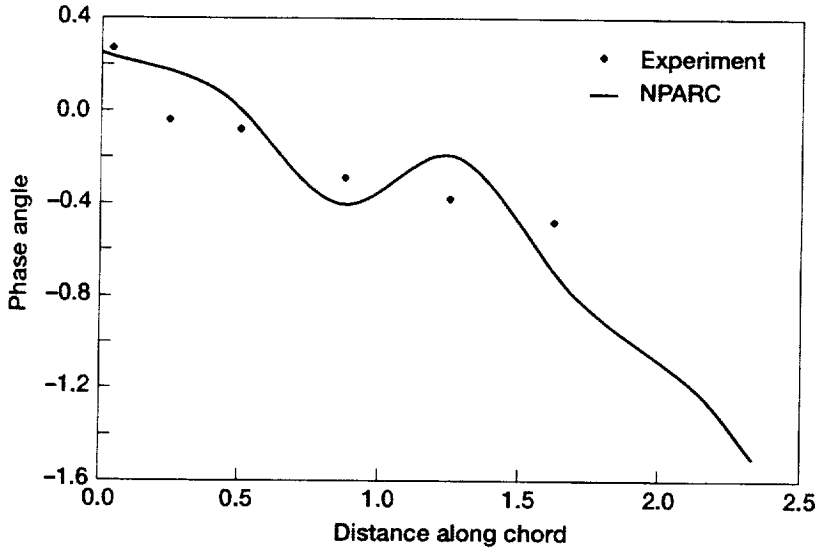

Figure 21.—Phase angle distribution on pressure surface (M_1 = 0.27, i = 2.98°).

REPORT DOCUMENTATION PAGE

Form Approved
OMB No. 0704-0188

1. AGENCY USE ONLY (*Leave blank*)	2. REPORT DATE	3. REPORT TYPE AND DATES COVERED
	January 2001	Technical Memorandum

4. TITLE AND SUBTITLE

Gust Response Analysis of a Turbine Cascade

5. FUNDING NUMBERS

WU–323–71–00–00

6. AUTHOR(S)

R.S.R. Gorla, T.S.R. Reddy, D.R. Reddy, and A.P. Kurkov

7. PERFORMING ORGANIZATION NAME(S) AND ADDRESS(ES)

National Aeronautics and Space Administration
John H. Glenn Research Center at Lewis Field
Cleveland, Ohio 44135–3191

8. PERFORMING ORGANIZATION REPORT NUMBER

E–12520

9. SPONSORING/MONITORING AGENCY NAME(S) AND ADDRESS(ES)

National Aeronautics and Space Administration
Washington, DC 20546–0001

10. SPONSORING/MONITORING AGENCY REPORT NUMBER

NASA TM—2001-210562

11. SUPPLEMENTARY NOTES

Prepared for the 46th International Gas Turbine and Aeroengine Technical Congress, Exposition, and Users Symposium sponsored by the American Society of Mechanical Engineers, New Orleans, Louisiana, June 4–6, 2001. R.S.R. Gorla, Department of Mechanical Engineering, Cleveland State University, Cleveland, Ohio 44115; T.S.R. Reddy, Department of Mechanical Engineering, The University of Toledo, Toledo, Ohio 43606; D.R. Reddy and A.P. Kurkov, NASA Glenn Research Center. Responsible person, D.R. Reddy, organization code 5430, 216–433–8133.

12a. DISTRIBUTION/AVAILABILITY STATEMENT

Unclassified - Unlimited
Subject Categories: 02 and 07 Distribution: Nonstandard

Available electronically at http://gltrs.grc.nasa.gov/GLTRS

This publication is available from the NASA Center for AeroSpace Information, 301–621–0390.

12b. DISTRIBUTION CODE

13. ABSTRACT ***(Maximum 200 words)***

A study was made of the gust response of an annular turbine cascade using a two-dimensional Navier Stokes code. The time-marching CFD code, NPARC, was used to calculate the unsteady forces due to the fluid flow. The computational results were compared with a previously published experimental data for the annular cascade reported in the literature. Reduced frequency, Mach number and angle of incidence were varied independently and the gust velocity was sinusoidal. For the high inlet velocity case, the cascade was nearly choked.

14. SUBJECT TERMS

Unsteady aerodynamics; Gust response; Turbine cascade

15. NUMBER OF PAGES

22

16. PRICE CODE

A03

17. SECURITY CLASSIFICATION OF REPORT	18. SECURITY CLASSIFICATION OF THIS PAGE	19. SECURITY CLASSIFICATION OF ABSTRACT	20. LIMITATION OF ABSTRACT
Unclassified	Unclassified	Unclassified	